Earthq Eng & Eng Vib (2016) 15: 607-616 **DOI**:10.1007/s11803-016-0347-8

Damage assessment for seismic response of recycled concrete filled steel tube columns

Huang Yijie[1, 2†], Xiao Jianzhuang[1‡] and Shen Luming[3§]

1. *Department of Structural Engineering, Tongji University, Shanghai 200092, China*
2. *Department of Civil Engineering, Shandong University of Science and Technology, Qingdao, China*
3. *School of Civil Engineering, University of Sydney, NSW 2006, Australia*

Abstract: A model for evaluating structural damage of recycled aggregate concrete filled steel tube (RCFST) columns under seismic effects is proposed in this paper. The proposed model takes the lateral deformation and the effect of repeated cyclic loading into account. Available test results were collected and utilized to calibrate the parameters of the proposed model. A seismic test for six RCFST columns was also performed to validate the proposed damage assessment model. The main test parameters were the recycled coarse aggregate (RCA) replacement percentage and the bond-slip property. The test results indicated that the seismic performance of the RCFST member depends on the RCA contents and their damage index increases as the RCA replacement percentage increases. It is also indicated that the damage degree of RCFST changes with the variation of the RCA replacement percentage. Finally, comparisons between the RCA contents, lateral deformation ratio and damage degree were implemented. It is suggested that an improvement procedure should be implemented in order to compensate for the performance difference between the RCFST and normal concrete filled steel tubes (CFST).

Keywords: recycled aggregate concrete (RAC); recycled concrete filled steel tube (RCFST); column; seismic performance; damage assessment model (DAM)

1 Introduction

Recycled aggregate concrete (RAC) is an environmentally friendly concrete that uses either partial or complete large aggregates collected from crushed waste concrete as its coarse aggregates. With an emphasis on the sustainability and conservation of natural resources, there has been increasing interest in the structural application of RAC as an alternative to conventional concrete (Tam *et al*., 2005; Topcu and Guncan, 1995). However, the wide application of RAC in engineering is somehow restricted due to its degraded properties when compared with conventional concrete. For example, RAC normally has slower strength development process (Xiao *et al*., 2012a; Poon *et al*., 2004), lower elastic modulus and strength (Amnon, 2003; Topcu and Sengel, 2004), higher shrinkage, creep and thermal conductivity (Hansen and Boegh, 1985; Etxeberria *et al*., 2007), and lower durability (Otsuki *et al*., 2003; Rohi *et al*., 2003) than normal concrete. The main reasons for the reduced property of RAC are: (1) the recycled aggregates used in RAC are composites and normally consist of natural crushed stones, attached old mortar and some impurities such as pieces of bricks (Xiao *et al*., 2012a); and (2) the weak interfacial transition zone (ITZ) between the original coarse aggregate and old cement paste can negatively affect the properties of RAC (Xiao *et al*., 2012a); and (3) the manufacturing process can damage the recycled coarse aggregates (RCA) (Nagatakia *et al*., 2004).

In order to compensate for the property differences between the RAC and normal concrete, confinement is usually applied to the RAC. Concrete-filled steel tubes (CFST) have gained wide acceptance due to their excellent outcomes (Hu *et al*., 2003). Composite action is achieved by the interaction of outer tube and core concrete. The infilled concrete could delay the local buckling of the steel tube, which can improve the mechanical behavior of members under various loading conditions (Hu *et al*., 2003). On the other hand, the steel tube not only works as a longitudinal reinforcement to resist the axial load and moment, but also as transverse reinforcement to confine the concrete and enhance the shear strength (Zhang *et al*., 2009). Hence, the recycled concrete filled steel tube (RCFST) may be considered as an excellent development to fulfill the wide acceptance of

Correspondence to: Xiao Jianzhuang, Department of Structural Engineering, Tongji University, Shanghai 200092, China
Tel: +86 021 65982787; Fax: +86 021 65986345
E-mail: jzx@tongji.edu.cn
†Lecturer; ‡Professor; §Associate Professor

Supported by: the National Natural Science Foundation of China under Grant Nos. 51408346 and 51438007, and the Shanghai Science and Technique Committee under Grant No. 14231201300
Received March 15, 2015; **Accepted** July 28, 2015

RAC in the construction industry. As a result, increasing interest has been given to the mechanical behavior of the RCFST. Konno *et al*. (1998), Xiao *et al*. (2012b) and Yang and Han (2006) have studied RCFST specimens under different static loading conditions. These test results showed that the mechanical behavior of RAC infilled steel tubes is similar to that of normal concrete infilled steel tubes. However, for specimens with the same material strength (core concrete strength and steel tube strength), the seismic performance of RCFST varies with the variation of recycled coarse aggregate replacement percentage. According to the test results from Han *et al*. (2003), Wu *et al*. (2013) and Xiao *et al*. (2014), the bearing capacity and stiffness degradation of RCFST decreases as the RCA content increases under seismic loading conditions. This phenomenon can be attributed to the fact that the damage of core RAC is more severe than that of core normal concrete under the same seismic loading history due to (1) the inferior ITZ between the original coarse aggregate and the old cement paste, and (2) the initial damage of RCA during the recycle processing. With increasing loads, the more serious damage of RAC leads to inferior seismic performance of the RCFST when compared to the CFST. Hence, a damage assessment method (DAM) needs to be developed in order to evaluate the damage evolution of a RCFST specimen, and to determine the seismic performance differences between the members of RCFST and CFST.

The DAM was first utilized by Shibata and Sozen (1974) to evaluate the seismic performance of engineering structures. Since then, Graham and Rakesh (1988), Park and Ang (1985a, 1985b), Fillipou *et al*. (1986), Wang and Shan (1987), Kunnath *et al*. (1990), Julio (1995) and Perera *et al*. (2000) have proposed different DAMs to evaluate the performance of structures/members under simulated earthquake conditions. These research findings have been applied to the design of reinforced concrete structures under earthquake conditions and have changed the structure design concept. However, all the above DAMs were focused on the reinforced concrete components, while the assessment method for the CFST is still not well developed (Zhang *et al*., 2009; Qiu *et al*., 1996; Chai, 1996). To the best knowledge of the authors, there is very few research work on the RCFST damage assessment. This situation needs to be improved as the CFST and RCFST have been used as important structural components (e.g., bridge piers and frame columns) and structures (e.g., long-span bridges and high-rise buildings). An accurate DAM could reflect the CFST/ RCFST performance during the loading history and provide guidelines for design.

In this study, a damage assessment model is developed to evaluate the potential damage of RCFST/CFST components as a function of the lateral deformation and the absorbed hysteretic energy (Park and Ang, 1985a). In order to develop a reasonable damage function, available test results were examined. Regression and theoretical analysis methods were used to calibrate the values of the parameters of the proposed damage model. Furthermore, a low frequency cyclic lateral load test was performed to study the damage evolution of specimens. The test results were used to validate the proposed DAM.

2 Damage model

Consistent with the dynamic behavior of the RCFST described earlier (Yang *et al*., 2009), seismic structural damage is expressed as a combination of the performance loss caused by deformation and repeated cyclic loading effect. This can be expressed by a damage index:

$$D=\sum_{j=1}^{n}D_j=\sum_{j=1}^{n}(\sum_{i}^{m}(\frac{E_{\mathrm{c}}^{i}}{E_{\mathrm{cf}}^{j}})) \tag{1}$$

where D_j is the damage index of the *j*th cyclic lateral displacement, E_{cf}^{j} is the absorbed hysteretic energy capacity of the *j*th lateral displacement and is related to the specimen lateral deformation and specimens details, and E_{c}^{i} is the hysteretic energy of the *i*th cyclic loading at *j*th lateral displacement (the meaning of *i*, *j*, *m*, *n* is shown in Fig. 1).

Values of the damage index, *D*, are such that $D \geq 1$ indicates destruction or serious damage to the specimen. Structural damage, therefore, *D* is a function of the response E_{c}^{i}; which is dependent on the loading history, whereas E_{cf}^{j} is independent on the loading history. In Eq. (1), the cyclic loading effect at different deformation levels is taken into account.

3 Determination of model parameter

The damage model proposed in Eq. (1) contains the E_{cf}^{j}, which needs to be calibrated using available experimental data. As mentioned earlier, E_{cf}^{j} is related to the specimen lateral deformation and specimen details. In general, the E_{cf}^{j} can be expressed as:

$$E_{\mathrm{cf}}^{j}=N_{\mathrm{f}}^{j}\times E_{\mathrm{ch}}^{j} \tag{2}$$

where N_{f}^{j} is the number of complete cycles to failure at the *j*th cyclic lateral displacement, and E_{ch}^{j} is the average hysteretic energy per cycle at the *j*th lateral displacement.

3.1 Average hysteretic energy per cycle

According to McCabe and Hall (1989), Park and Ang (1985a), Chai (1996), Zhang *et al*. (2009) and Qiu *et al*. (1996), E_{ch}^{j} can be evaluated. In the evaluation, E_{ch}^{j} is related to the lateral deformation ratio (μ),yield load of specimen (P_{y}),yield deformation (Δ_{y}), and other factors, and can be expressed as follows (yield load of the specimen is defined as the load at which the steel tube begins to deform plastically. Prior to the yield load, the material deforms elastically.):

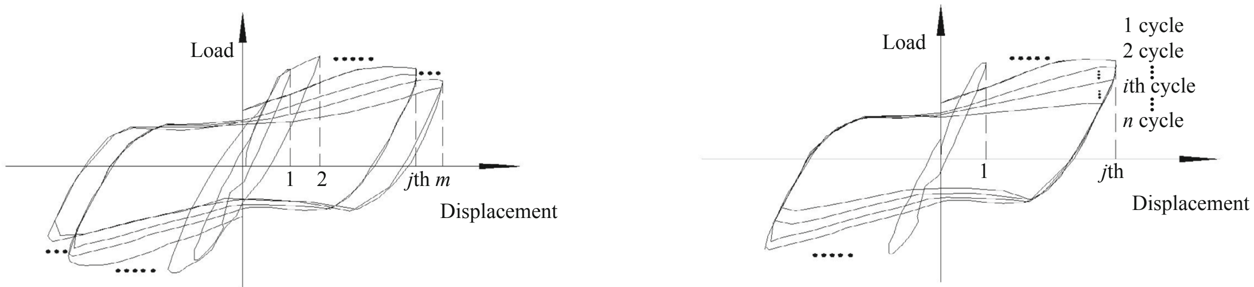

(a) Illustration of *j* and *m* (a) Illustration of *i* and *n*

Fig. 1 Illustration of *i*, *j*, *m* and *n*

$$E_{\mathrm{ch}}^{j} = 2P_{\mathrm{y}}\Delta \qquad \mu \geq 2 \tag{3}$$

$$E_{\mathrm{ch}}^{j} = 2P_{\mathrm{y}}\Delta_{\mathrm{y}}[(0.5+2.34\frac{\Delta_{\mathrm{f}}}{\Delta_{\mathrm{y}}})(\mu-1)+(0.78-1.54\frac{\Delta_{\mathrm{f}}}{\Delta_{\mathrm{y}}})] \qquad 1.5 \leq \mu < 2 \tag{4}$$

where Δ is the jth lateral displacement, $\mu = \Delta/\Delta_{\mathrm{y}}$ is the lateral deformation ratio, Δ_{f} is the flexural component of the yielding deformation (Δ_{y}) and $\frac{\Delta_{\mathrm{f}}}{\Delta_{\mathrm{y}}} = 0.9$ is used for most cases.

For the lateral displacement in the range of $0 \leq \Delta/\Delta_{\mathrm{y}} < 1.5$, there is a lack of available data that can be used to evaluate the hysteretic energy E_{cf}^{j} of the RCFST specimen. However, based on the work of Amir *et al*. (2004), it can be assumed that the composite action between the steel tube and the core concrete is relatively small before the specimens yields, and the behavior of CFST/RCFST is similar to that of reinforced concrete members. Hence, it is hypothesized that before the specimens yields, E_{ch}^{j} can be expressed as Eq. (5) according to Park and Ang (1985a):

$$E_{\mathrm{Ch}}^{j} = (0.77\mu - 0.22)P_{\mathrm{y}}\Delta_{\mathrm{y}} \qquad 0 \leq \mu < 1 \tag{5}$$

and E_{ch}^{j} can be calculated by the linear interpolation for $1 \leq \Delta/\Delta_{\mathrm{y}} < 1.5$.

According to Eqs. (3)−(5), the average hysteretic energy per cycle at the jth lateral displacement E_{ch}^{j} can be evaluated when the yield load P_{y}, yield deformation Δ_{y} and ductility factor are obtained. The parameters in Eqs. (3)−(5) can be calculated as follows.

3.1.1 Yield load

The yield load (P_{y}) of CFST/RCFST can be evaluated based on the standard text book (Eurocode 4 for composite steel and concrete structures, 2004; Han, 2007) and the test results (Yang *et al*., 2009; Wu *et al*., 2013; Xiao *et al*., 2014). The expression for P_{y} is given by:

$$P_{\mathrm{y}} = \begin{cases} 1.05a(0.82+0.03r)(1-0.03r)\psi\gamma_{\mathrm{m}}W_{\mathrm{sm}}f_{\mathrm{smy}}/L_1 & 1<\xi\leq 4 \\ a(0.82+0.03r)(1-0.03r)(0.2\xi+0.85)\psi\gamma_{\mathrm{m}}W_{\mathrm{sm}}f_{\mathrm{smy}}/L_1 & 0.2<\xi\leq 1 \end{cases} \tag{6a}$$

$$f_{\mathrm{smy}} = \left[1.212+(0.18\frac{f_{\mathrm{y}}}{235}+0.974)\xi+(-\frac{0.104f_{\mathrm{c}}}{20}+0.0309)\xi^2\right]f_{\mathrm{c}} \Big/ (1-0.4r^2+0.45r) \tag{6b}$$

where f_{y} represents the yield strength of the steel tube, f_{c} is the compressive strength of the core concrete, ϕ and L_1 are the diameter and 0.5 times the height of the structure components, respectively, with L_1 plotted in Fig. 2; $\xi = (f_{\mathrm{y}}A_{\mathrm{s}})/f_{\mathrm{c}}A_{\mathrm{c}}$ represents the constraint factor, n is the axial load ratio, r is the RCA replacement percentage, ψ is the axial load ratio parameter; and a, γ_{m}, W_{sm} are the parameters that can be found in Han (2007).

The yield load of the specimen (P_{y})can therefore be calculated with Eqs. (6a)−(6b) when the details of specimen (f_{y}, f_{c} and ϕ etc.) are given. In Eqs. (6a)−(6b), note that the influence of the RCA replacement percentage is considered. That is because the mechanical behavior of RCFST varies with the changes of RCA contents. A comparison between the experimental results (Qiu *et al*., 1996; Yang *et al*., 2009; Xiao *et al*., 2014; Zhang, 2009; Zhang *et al*., 2014; Amir *et al*., 2004; Wu *et al*., 2013.) and the calculated ones is shown in Fig. 3. It can be found that the data associated with Eq. (6) is not scatter, with a correlation coefficient of 98.2%. The covariance about Eq. (6) is greater than zero, which

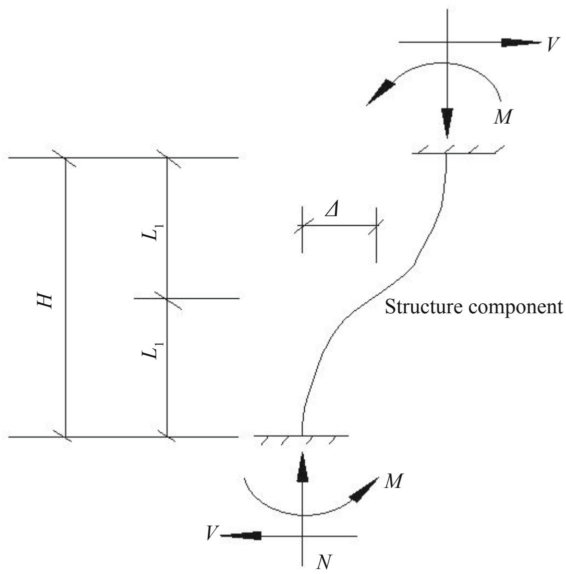

Fig. 2 Illustration of L_1

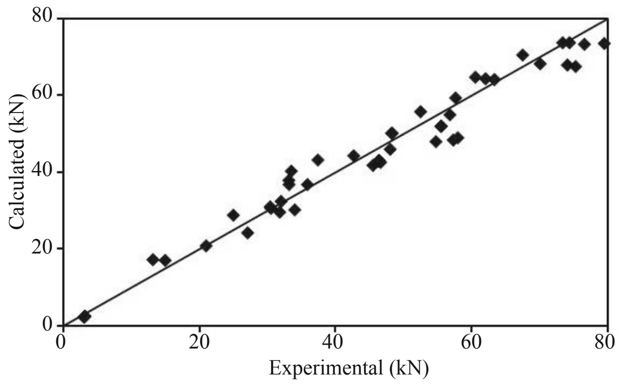

Fig. 3 Comparison between calculated and experimental yield load

indicates that the calculated P_y is in agreement with the experimental results.

3.1.2 Yield deformation

The method for evaluating the yield deformation of the member, Δ_y, may be found in the standard text book (Eurocode 4 for composite steel and concrete structures, 2004; Han, 2007). To calculate Δ_y of the concrete/RAC infilled steel tube subjected to reversed loadings, the following equations are proposed based on the analysis of the test results and the related references (Yang *et al*., 2009; Qiu *et al*., 1996; Han *et al*., 2003).

$$\Delta_y = \frac{P_y L_1^3}{3K_{em}} \tag{7a}$$

$$K_{em} = 0.16(1-0.05r)\frac{(1-0.03r)\gamma_m W_{sm} f_{smy}}{\varphi_e} \tag{7b}$$

$$\varphi_e = [(4.25\beta_c + 100.14) + (15.8\beta_c + 3.65)\xi]\beta_s^{0.82} / (E_s \phi) \tag{7c}$$

where f_{cu} is the cube compressive strength of core concrete and E_s represents the elastic modulus of the steel tube; and β_s and β_c are parameters that can be found in Han (2007). It is also found from Eqs. (7a)−(7c) that the effect of the RCA contents is considered.

Using Eqs. (7a)−(7c), the yield deformation of specimen (Δ_y) is calculated for 38 specimens. The comparison between the experimental and calculated ones is shown in Fig. 4 (Qiu *et al*., 1996; Yang *et al*., 2009; Xiao *et al*., 2014; Zhang *et al*., 2014; Amir *et al*., 2004, Wu *et al*., 2013.). The correlation coefficient about Eqs. (7a)−(7c) is approximately 98.4%, indicating the data are not scatter. The covariance about Eq. (7) is greater than zero.

3.2 Number of complete cycles

N_f^j is the number of complete cycles to failure at the *j*th cyclic lateral displacement. According to the experimental data from Qiu *et al*. (1996), N_f^j is related to the lateral displacement Δ. However, Zhang *et al*. (2009) concluded that N_f^j is a function of the diameter to thickness ratio, lateral displacement, and so on. Based on the available experimental results (Qiu *et al*., 1996; Zhang *et al*., 2009.), the following relation can be obtained based on the diameter to thickness ratio (ϕ / t) and lateral deformation:

$$\delta = 20 \times [\ln(\phi / t)]^{0.2309} \times (2N_f^j)^{-0.1519\times\ln(\phi/t)} \tag{8}$$

$$\delta = \frac{\Delta}{L_1} \times 100\% \tag{9}$$

where L_1 is a half of the structure member's height.

3.3 Calculated results compared with test results

The absorbed hysteretic energy capacity at the *j*th lateral displacement (E_{cf}^j) can be evaluated when both N_f^j and E_{ch}^j are fixed. The comparison between the calculated E_{cf}^j and the corresponding experimental data (Zhang *et al*., 2009; Qiu *et al*., 1996) is shown in Fig. 5. It is found from the figure that the calculated ones are in agreement with the experimental results, and the data associated with Eq. (2) are not scatter with a correlation coefficient of 98%, and covariance about Eq. (2) is greater than zero. Hence, Eqs. (2) can be employed to evaluate the absorbed energy capacity of CFST/RCFST under seismic conditions.

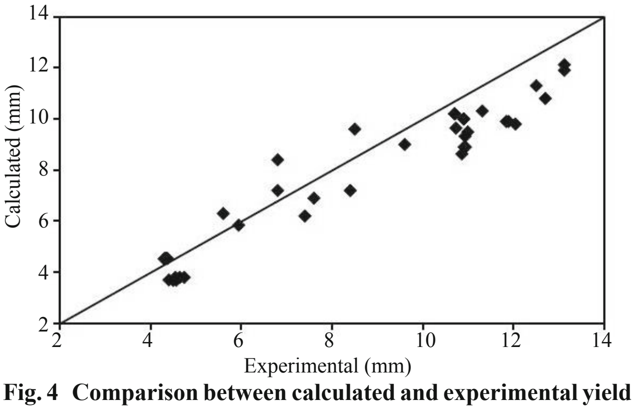

Fig. 4 Comparison between calculated and experimental yield deformation

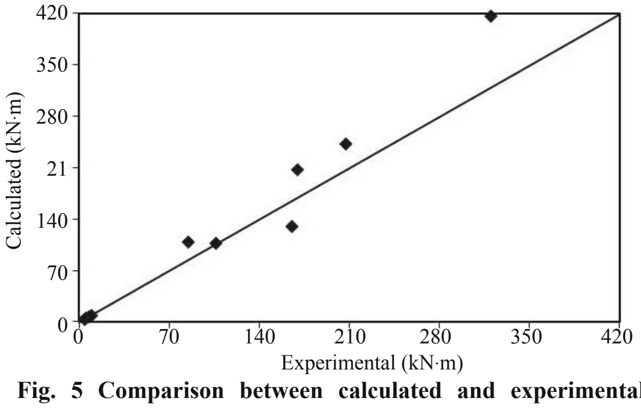

Fig. 5 Comparison between calculated and experimental absorbed energy

Based on the proposed damage model (Eq. (1)), the damage evaluation of RCFST/CFST under seismic conditions can be performed when E_{cf}^{j} and E_{c}^{i} are obtained. As mentioned before, E_{c}^{i} is dependent on the loading history, whereas E_{cf}^{j} is independent of the loading history. In order to obtain the damage conditions of RCFST/CFST under different displacement levels, a seismic test needs to be carried out.

4 Seismic damage assessment of RCFST

4.1 Experiment and results

In order to evaluate the damage evolution of CFST/RCFST under seismic conditions, six large-scale RCFST columns under low frequency cyclic lateral loads were tested. The main parameter in this study is the RCA replacement percentage (the properties of coarse aggregates are shown in Table 1). The loading setup and the arrangement of linear voltage displacement transducers (LVDTs) are shown in Fig. 6. The details of the specimens are reported in Table 2. The typical hysteresis curves are also shown in Fig. 7. It can be found from the figure that all the hysteresis shapes are rounded, which indicates that the columns have excellent energy absorbing capacity. The shape of the hysteretic loops of the specimens with RAC is similar to that of the specimen with normal concrete. Other details about the experiments can be found in Xiao *et al*. (2014).

Generally, the stiffness degeneration is used to reflect the damage evolution of the specimen. Figure 8 shows the stiffness degeneration law of the specimen. It can be found that the specimen stiffness decreases as the lateral deformation increases, which indicates that the seismic performance of the specimen decreases and the damage increases. However, it is hard to investigate the effect of RAC on the damage evolution of the specimen from Fig. 8. Hence, the proposed damage assessment model is used to represent the damage evolution.

4.2 Damage evaluation

(1) Lateral deformation influence

Based on the above experimental data and the proposed damage model (Eqs. (1)−(9)), the damage evolution of RCFST under simulated seismic conditions is shown in Fig. 9. It is found that the damage index of the specimen increases as the lateral deformation increases. The damage index is negligible when the lateral deformation is relatively small ($\Delta \le 0.02L$); after that, the value of D increases rapidly.

The damage values at different lateral deformation levels are also given in Table 3. It can be found that the damage value D is less than 0.2 for $\Delta \le \frac{L}{50}$ (L is the specimen height). After that, the damage increases rapidly. For $\Delta \ge \frac{L}{20}$, D is greater than 1, which represents the failure of specimen. These analysis results

Table 1 Basic properties of recycled coarse aggregate and natural coarse aggregate

	Size (mm)	Bulk density kg·m^{-3}	Apparent density (kg·m^{-3})	Clay dosage (%)	Water absorption (%)
RCA	5−31.5	1320	2500	3.5	5.60
NCA	5−31.5	1410	2620	-	0.51

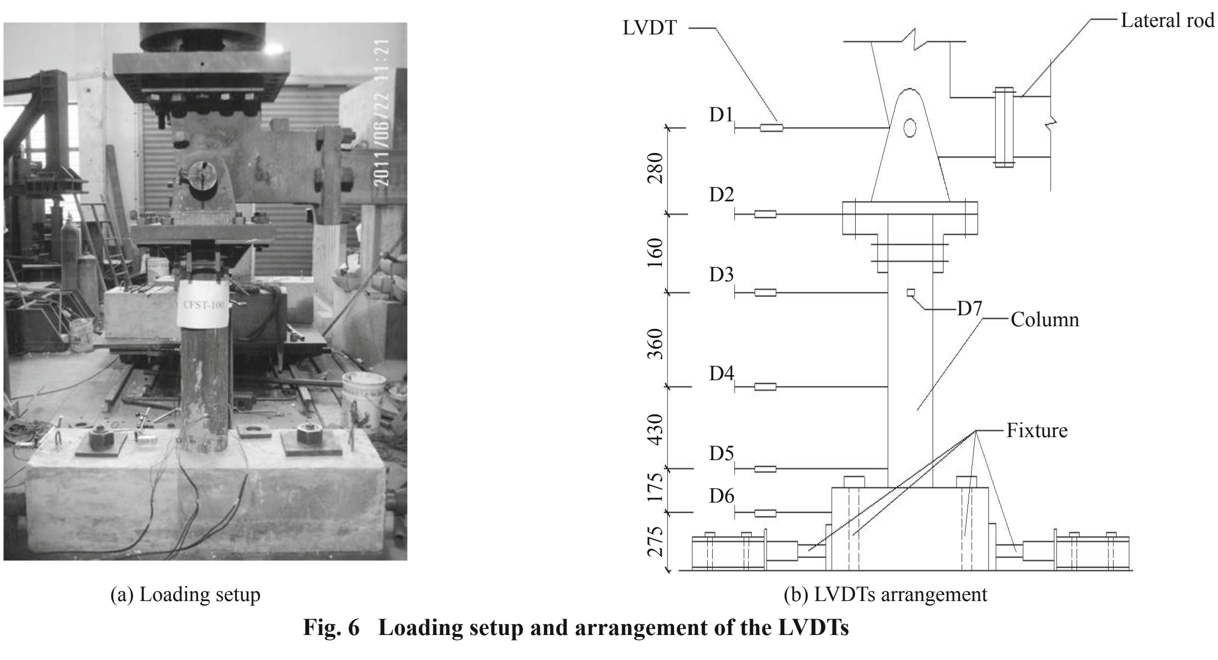

(a) Loading setup (b) LVDTs arrangement

Fig. 6 Loading setup and arrangement of the LVDTs

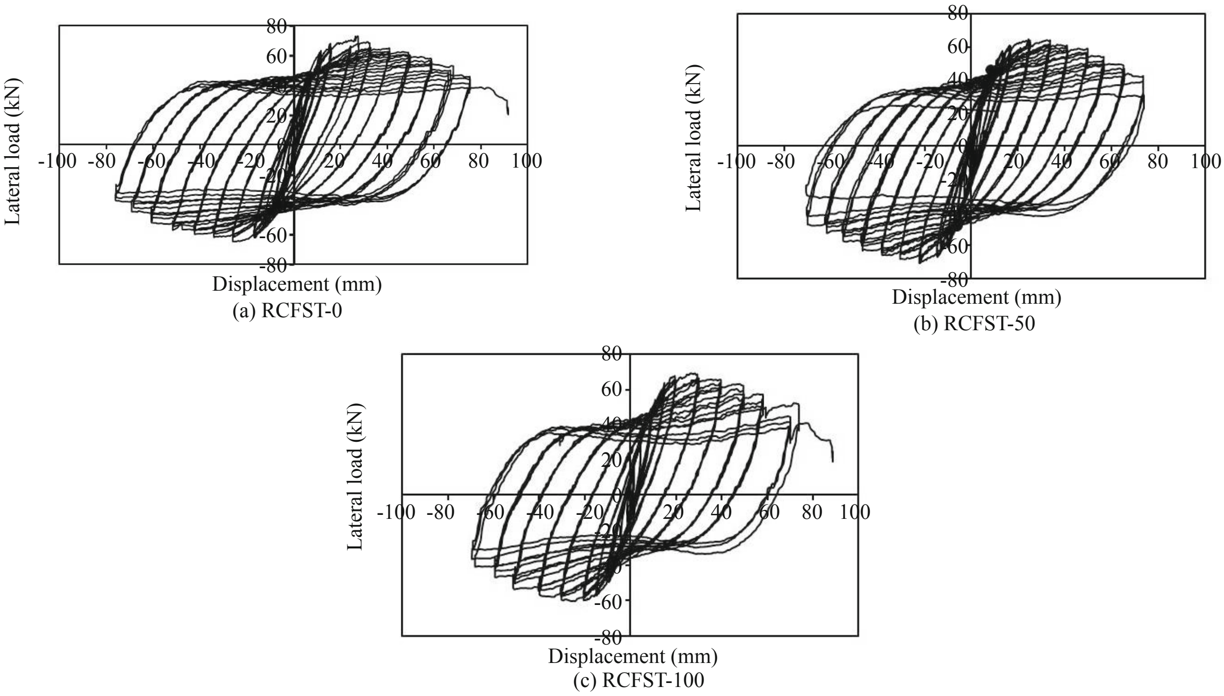

Fig. 7 Hysteresis curves

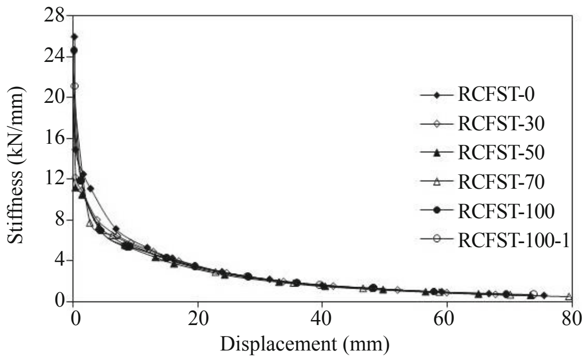

Fig. 8 Stiffness degradation of RCFST under cyclic loading

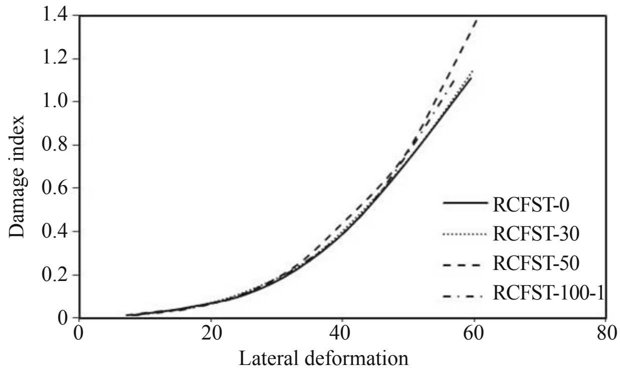

Fig. 9 Damage evolution of RCFST under cyclic loading

Table 2 Specimen details

Specimen	RCA replacement percentage (%)	D (mm)	t (mm)	f_{cu} (N/mm^2)	L (mm)
RCFST-0	0	220	4	29	1280
RCFST-30	30	220	4	25	1280
RCFST-50	50	220	4	25	1280
RCFST-70	70	220	4	29	1280
RCFST-100	100	220	4	28	1280
RCFST-100-1	100	220	4	28	1280

Table 3 Damage index under different lateral displacement

Lateral deformation	D					
	RCFST-0	RCFST -30	RCFST -50	RCFST -70	RCFST -100	RCFST -100-1
L/500	0.002	0.0021	0.002	0.0018	0.0019	0.0019
L/100	0.03	0.028	0.031	0.053	0.043	0.026
L/50	0.115	0.116	0.127	0.179	0.155	0.118
L/25	0.780	0.794	0.913	0.781	0.710	0.841
L/20	>1	>1	>1	>1	>1	>1

are in agreement with the experimental data. During the test, the specimen was in the elasto-plastic stage when the lateral deformation was less than 0.02L, which indicated that the damage of the specimen was relatively small. However, when the lateral deformation was about 0.05−0.06L, the outer steel tube began to fracture at the end of the column and the bearing capacity was about 80% of the peak value. The typical phenomenon of the specimens at different lateral displacement levels is shown in Fig. 10.

(2) RCA replacement percentage

The recycled coarse aggregate replacement percentage has influence on the damage evolution of the specimen because the damage index of RCFST is larger than that of CFST (RCFST-0) under the same lateral deformation (Fig. 9). The damage index of RCFST increases more rapidly than that of CFST. Under the same conditions, the damage index increases as the recycled coarse aggregate replacement percentage increases, which suggests that the seismic performance of the specimens with RAC deteriorate more severely than those with normal concrete.

It can be also found from the Table 3 that the difference between the damage index of RCFST and that of CFST increases as the lateral displacement Δ_l and RCA contents increases. The difference between the damage index of RCFST-0 and those of other RCFSTs is relatively small at the initial stage of the test. When Δ_l= 0.02L, the damage index of RCFST-0 is 0.9%, 10.4% and 2.6% lower than those of RCFST-30, RCFST-50 and RCFST-100-1, respectively. However, the damage index of RCFST-0 is 1.8%, 17.1% and 7.8% lower than those of RCFST-30, RCFST-50 and RCFST-100-1 for Δ_l= 0.05L, respectively.

4.3 Damage degree

Park and Ang (1985b) divided the degree of reinforced concrete structural damage into five categories: slight, minor, moderate, severe and collapse. Every damage degree has a certain range within the damage index. For example, the damage index for slight degree ranges from 0 to 0.2. Based on Parks' analysis and conclusions, the results shown in Table 4 serve to calibrate the damage degree (damage index) of RCFST. It is found that, under the same damage degree (damage index), the lateral deformation ratio (Δ/Δ_y) decreases as the RCA replacement percentage increases, which means that the damage degree (damage index) of RCFST is more serious than that of CFST under the same Δ/Δ_y. Therefore,

(a) Δ = 0.02L

(b) Δ = 0.05L

Fig. 10 Experimental phenomenon of RCFST-50 under different lateral displacement levels

Table 4 Damage degree

Description	RCFST-0	RCFST -30	RCFST -50	RCFST -70	RCFST -100-1
Lateral deformation	$< \Delta_y$	$< \Delta_y$	$< \Delta_y$	$< \Delta_y$	$< \Delta_y$
Damage degree ($D \approx 0$)			None		
Lateral deformation	$< 2.5\Delta_y$	$< 2.48\Delta_y$	$< 2.44\Delta_y$	$< 2.28\Delta_y$	$< 2\Delta_y$
Damage degree ($D \le 0.1$)			Slight		
Lateral deformation	$4\Delta_y$	$3.91\Delta_y$	$3.66\Delta_y$	$3.66\Delta_y$	$3.64\Delta_y$
Damage degree ($D \le 0.4$)			Minor		
Lateral deformation	$4.87\Delta_y$	$4.73\Delta_y$	$4.35\Delta_y$	$4.55\Delta_y$	$4.36\Delta_y$
Damage degree ($D \le 0.6$)			Moderate		
Lateral deformation	$5.68\Delta_y$	$5.66\Delta_y$	$5.04\Delta_y$	$5.41\Delta_y$	$5.09\Delta_y$
Damage degree ($D \le 0.8$)			Severe		
Lateral deformation	$6.24\Delta_y$	$6.06\Delta_y$	$5.68\Delta_y$	$6.04\Delta_y$	$5.6\Delta_y$
Damage degree ($D \ge 1$)			Damage		

in order to make the seismic performance of RCFST equivalent to that of CFST, some improvements are needed. According to Eqs. (2)−(9), the best method is to change the specimen diameter to thickness ratio (ϕ / t).

4.4 Procedure of RCFST columns damage assessment

The details about this procedure are described as follows:

(1) Determine the parameters of the RCFST columns (diameter, material strength, height and tube thickness, etc.);

(2) Calculate the characteristic parameters of RCFST columns (yield load, yield deformation and average hysteretic energy per cycles) by using Eqs. (3)−(7);

(3) Fix the response of the RCFST columns (lateral deformation, load and energy, etc.) under seismic conditions by field measurement or numerical simulation (ANSYS, ABAQUS and SAP, etc.);

(4) Calculate the characteristic parameters of the RCFS columns (complete cycle numbers) by using Eqs. (8)−(9) and the response of the RCFST columns.

(5) Use Eqs. (1)−(2) and the response of RCFST columns to determine the damage degree (index) of the columns.

5 Conclusions

In this study, a damage assessment model is developed to evaluate the structural damage of a recycled aggregate concrete filled steel tube (RCFST) under seismic loading. The following conclusions can be drawn.

(1) The RCA replacement percentage has a slight influence on the damage evolution of the columns. The damage index increases as the RCA contents increases under the same lateral deformation. The damage index of the RCFST increases more rapidly than that of a CFST.

(2) The effect of lateral displacement on the seismic performance of the specimens is obvious. The damage evolution of the RCFST increases as the lateral deformation increases. The damage index is negligible when the lateral deformation is small; after that, the damage index increases rapidly.

(3) Based on the test results, the relationship between the damage degree, RCA replacement percentage and the lateral deformation ratio is established. The damage assessment procedure for RCFST columns is also suggested. Under the same damage degree conditions, the lateral deformation ratio decreases as the RCA replacement percentage increases. Thus, some methods need to be carried out to improve the seismic performance of RCFST.

Acknowledgment

This work was sponsored by the National Natural Science Foundation of China (Grant No. 51408346, 51438007), and the Shanghai Science & Technique Committee (Grant No. 14231201300)

References

Amir F, Frank SQ and Sami R (2004), "Concrete-filled Steel Tubes Subjected to Axial Compression and Lateral Cyclic Loads," *Journal of Structural Engineering*, **130**(4): 631−640.

Amnon K (2003), "Properties of Concrete Made with Recycled Aggregate from Partially Hydrated Old Concrete," *Cement and Concrete Research*, **33**(5): 703−711.

Chai YH (1996), "An Analysis of the Seismic Characteristic of Steel-jacketed Circular Bridge Columns," *Earthquake Engineering and Structural Dynamics*, **25**(2): 149−161.

Etxeberria M, Vázquez E, Marí A and Barra M (2007), "Influence of Amount of Recycled Coarse Aggregates and Production Process on Properties of Recycled Aggregate Concrete," *Cement and Concrete Research*, **37**(5): 735−742.

Eurocode 4 (2004), *Design of Composite Steel and Concrete Structures-Part 1.1: General Rules and Rules for Buildings* (EN 1994−1−1).

Filippou FC, Popov EP and Bertero VV (1986), "Analytical Studies of Hysteretic Behavior of RC Joints," *Journal of the Structural Engineering*, **112**(7): 1605−1622.

Graham HP and Rakesh A (1988), "Seismic Damage Prediction by Deterministic Methods: Concepts and Procedures," *Earthquake Engineering and Structural Dynamics*, **16**(5): 719−734.

Han LH (2007), *The Concrete Filled Steel Tube Structures-theoretical and Practice*, Science Press, Beijing. (in Chinese)

Han LH, Yang YF and Tao Z (2003), "Concrete Filled Thin Walled Steel RHS Beam-columns Subjected to Cyclic Loading," *Thin Walled Structures*, **41**(9): 801−833.

Hansen TC and Boegh E (1985), "Elasticity and Drying Shrinkage of Recycled Aggregate Concrete," *ACI Journal*, **82**(5): 648−652.

Hu HT, Huang CS, Wu MH and Wu YM (2003), "Nonlinear Analysis of Axially Loaded Concrete Filled Tube Columns with Confinement Effect," *Journal of*

Structural Engineering, **129**(10): 1322−1329.

Julio FL (1995), "Simplified Model of Unilateral Damage for RC Frames," *Journal of Structural Engineering*, **121**(12): 1765−1772.

Konno K, Sato Y, Kakuta Y and Ohira M (1998), "Property of Recycled Concrete Column Encased by Steel Tube Subjected to Axial Compression," *Transactions of the Japan Concrete Institute*, **19**(2): 231−238.

Kunnath SK, Reinhorn AM and Park YJ (1990), "Analytical Modeling of Inelastic Seismic Response of RC Structure," *Journal of the Structural Engineering*, **116**(4): 996−1017.

McCabe SL and Hall WJ (1989), "Assessment of Seismic Structural Damage," *Journal of Structural Engineering*, **115**(9): 2166−2183.

Nagatakia S, Gokceb A, Saekic T and Hisadad M (2004), "Assessment of Recycling Process Induced Damage Sensitivity of Recycled Concrete Aggregates," *Cement and Concrete Research*, **34**(6): 965−971.

Otsuki N, Miyazato S and Yodsudjai W (2003), "Influence of Recycled Aggregate on Interfacial Transition Zone, Strength, Chloride Penetration and Carbonation of Concrete," *Journal of Materials in Civil Engineering*, **15**(5): 443−451.

Park YJ and Ang HS (1985a), "Mechanic Seismic Damage Model for Reinforced Concrete," *Journal of Structural Engineering*, **111**(4): 722−739.

Park YJ and Ang HS (1985b), "Seismic Damage Analysis of Reinforced Concrete Building," *Journal of Structural Engineering*, **111**(4): 740−757.

Perera P, Alarcon ACE, *et al*. (2000), "A Fatigue Damage Model for Seismic Response of RC Structures," *Computers and Structures*, **78**(1−3): 293−302.

Poon CS, Shui ZH, Lam L, Fok H and Kou SC (2004), "Influence of Moisture States of Natural and Recycled Aggregates on the Slump and Compressive Strength of Concrete," *Cement and Concrete Research*, **34**(1): 31−36.

Qiu FW, Yang WD and Ou JP (1996), "Testing Research for the Dissipated Hysteric Energy and Accumulated Damage of CFST Column," *Journal of Harbin University of Civil Engineering and Architecture*, **29**(3): 41−45. (in Chinese)

Rohi MS, Burdette EG and Jackson NM (2003), "Resistance to Freezing and Thawing of Recycled Aggregate Concrete," *ACI Material Journal,* **100**(3): 216−221.

Shibata A and Sozen MA (1974), *The Substitute Structure Method for Earthquake-resistant Design of Reinforced Concrete Frames*, University of Illinois at Urbana-Champaign, Champaign.

Tam VWY, Gao XF and Tam CM (2005), "Micro Structural Analysis of Recycled Aggregate Concrete Produced from Two-stage Mixing Approach," *Cement and Concrete Research*, **35**(6): 1195−203.

Topcu IB and Guncan NF (1995), "Using Waste Concrete as Aggregate," *Cement and Concrete Research*, **25**(7): 1385−1390.

Topcu IB and Sengel S (2004), "Properties of Concretes Produced with Waste Concrete Aggregate," *Cement and Concrete Research*, **34**(8): 1307−1312.

Wang ML and Shan SP (1987), "Reinforced Concrete Hysteresis Model Based on the Damage Concept," *Earthquake Engineering and Structural Dynamics*, **15**(8): 993−1003.

Wu B, Zhao XY Zhang JS and Yang Y (2013), "Cyclic Testing of Thin-walled Circular Steel Tubular Columns Filled with Demolished Concrete Blocks and Fresh Concrete," *Thin-Walled Structures*, **66**: 50−67.

Xiao JZ, Huang YJ and Sun ZH (2014), "Seismic Behavior of Recycled Aggregate Concrete Filled Steel and Glass Fiber Reinforced Plastic Tube Columns," *Advances in Structural Engineering*, **17**(5): 693−707.

Xiao JZ, Huang YJ, Yang J and Zhang Ch (2012b), "Mechanical Properties of Confined Recycled Aggregate Concrete under Axial Compression," *Construction and Building Materials*, **26**(1): 591−603.

Xiao JZ, Li WG and Poon CS (2012a), "Recent Studies on Mechanical Properties of Recycled Aggregate Concrete in China-a Review," *Science China-Technological Sciences*, **55**(6):1463−1480.

Yang YF and Han LH (2006), "Experimental Behaviour of Recycled Aggregate Concrete Filled Steel Tubular Columns," *Journal of Constructional Steel Research*, **62**(12): 1310−1324.

Yang YF, Han LH and Zhu L (2009), "Experimental Performance of Recycled Aggregate Concrete Filled Circular Steel Tubular Columns Subjected to Cyclic Flexural Loadings," *Advances in Structural Engineering*, **12**(2): 183−1894.

Zhang GW (2009), *Research on Cumulative Seismic Damage of CFT Columns*, Hunan University, Changsha. (in Chinese)

Zhang GW, Xiao Y and Kunnath S (2009), "Low-cycle Fatigue Damage of Circular Concrete-filled-tube Columns," *ACI Structural Journal*, **106**(2): 151−159.

Zhang XG, Chen, ZP, Xue, JY and Su YS (2014), "Experimental Study on Seismic Behavior of Recycled Aggregate Concrete Filled Steel Tube Columns," *China Civil Engineering Journal*, **47**(9): 45−56. (in Chinese)

Appendix 1

Notation

A_c	Cross-sectional area of the core concrete
A_s	Cross-sectional area of the outer steel tube
ϕ	Outer steel tube diameter
D	Damage index
D_j	Damage index of the *j*th cyclic lateral displacement
E_s	Elastic modulus of steel
E^j_{cf}	Absorbed hysteretic energy capacity of the *j*th lateral displacement
E^j_{ch}	Averagely hysteretic energy per cycle at the *j*th lateral displacement
f_{cu}	Cube compressive strength of concrete
f_c	Axial compressive strength of plain RAC
f_y	Yield strength of steel
P_y	Yield load of specimen
N^j_f	Number of complete cycles to failure at the *j*th cyclic lateral displacement
n	Axial load ratio
r	RCA replacement percentage
L_1	0.5 times height of structure component
$a, \beta_s, \beta_c\, \gamma_m$	Parameters in the equations
μ	Lateral deformation ratio
ξ	Constraint factor
ψ	Axial load ratio parameter
Δ	*j*th lateral displacement
Δ_y	Yield deformation
Δ_f	Flexural component of the yield deformation

Appendix 2

The details of related experimental results are as follows.

	Specimen	D (mm)	t (mm)	f_{cu} (MPa)	N_o (kN)	P_y (kN)	Absorbed energy (kN·m)
Qiu *et al*. (1996)	1	40	1.5	30.0	20	31.2	4.0
	2	40	1.5	30.0	20	31.2	6.3
	3	40	1.5	30.0	20	31.2	4.8
	4	40	1.5	30.0	20	31.2	4.2
	5	40	1.5	30.0	30	32.5	3.7
	6	40	1.5	30.0	30	32.5	390
Zhang *et al*. (2009)	CFT110-C2-1	330	3.0	44.7	1300	-	131
	CFT110-C4	330	3.0	44.7	1300	-	108
	CFT110-C6-2	330	3.0	44.7	1300	-	109
	CFT57-C6	330	5.78	48.7	1300	-	209
	CFT57-C4	330	5.78	48.7	1300	-	242
	CFT57-C2	330	5.78	48.7	1300	-	419
Yang *et al*. (2009)	L0	165	2.57	60.4	62.8	63.3	-
	L1	165	2.57	59.2	62.1	62	-
	L2	165	2.57	52.2	57.7	60.5	-
	M0	165	2.57	60.4	313.9	75.2	-
	M1-1	165	2.57	59.2	310.3	74	-
	M1-2	165	2.57	59.2	310.3	73.2	-
	M2-1	165	2.57	52.2	288.7	69.4	-
	M2-2	165	2.57	52.2	288.7	73.3	-
	H0	165	2.57	60.4	600	79.4	-
	H1-1	165	2.57	59.2	600	75.9	-
	H1-2	165	2.57	59.2	600	77.3	-
	H2-1	165	2.57	52.2	600	74.3	-
	H2-2	165	2.57	52.2	600	72.2	-